

Effect of steam and oxygen starvation on severe accident progression with air ingress

Róbert Farkas^{a,*}, Zoltán Hózer^a, Imre Nagy^a, Nóra Vér^a, Márta Horváth^a, Martin Steinbrück^b, Juri Stuckert^b, Mirco Grosse^b

^a Centre for Energy Research (EK), Budapest, Hungary

^b Karlsruhe Institute of Technology (KIT), Karlsruhe, Germany

ARTICLE INFO

Keywords:

Severe accident test
Core degradation
VVER reactor

ABSTRACT

The CODEX-AIT-3 experiment simulated an in-vessel air ingress scenario after failure of bottom head of a nuclear reactor. 1600 °C maximum temperature was reached with the electrically heated bundle and slow cool-down was applied at the end of the test to demonstrate the bundle state before quench. Limited air and steam flow rates were intentionally selected in order to slow down the high temperature chemical interactions and provided unique data on nuclear fuel behaviour under oxygen and steam starvation conditions. The individual oxidation and nitriding phenomena were well separated from each other and it was indicated by the complex microstructures in the zirconium cladding with nitrides, oxides and transition zones. The competition between different chemical reactions could be excluded in some locations and some time periods. The post-test numerical analyses of the experiment could be used for the evaluation of the role of numerical models developed for individual chemical reactions in severe accident codes.

1. Introduction

Severe reactor accidents involve a large number of complex phenomena during different stages of core degradation. Due to high decay heat and low heat removal from the core, the fuel rods heat up, lose integrity and rod-like geometry. Physical and chemical interactions take place between core components at high temperatures (Hofmann, 1999; Dubourg et al., 2010; Adroguer et al., 2005). The fission products release from the fuel rods intensifies with the increase of temperature (Clément and Zeyen, 2013; Gallais-During et al., 2017; Pontillon et al., 2017).

The typical reactor core of a nuclear power plant is several meters high and several meters in diameter. During an accident, large differences can be created in the terms of power, temperature, coolant accessibility or starvation, which create a heterogeneous picture of degradation processes in a given moment. Melting of fuel rods can progress in the central part of the core, while some peripheral rods may still maintain rod-like geometry, as it was observed for example in the TMI-2 accident (McCardell et al., 1990).

The failure of reactor bottom head by the molten corium, severe accident in the spent fuel pool or in an open reactor may result in air access to hot fuel rods (Powers et al., 1994; Duriez et al., 2007). The

presence of oxygen and nitrogen in the atmosphere intensifies some chemical reactions, accelerates accident progression and may result in the enhancement of activity release through the formation of gaseous species, e.g. ruthenium oxides (Giordano et al., 2010; Ohnet et al., 2018; Mun et al., 2006; Auvinen et al., 2008). If there is continuous supply of air in the vicinity of the hot fuel rods, zirconium fire may take place.

The oxidation of zirconium alloys in air, oxygen or air-steam mixtures, and the direct chemical reaction of nitrogen with zirconium was addressed in several separate-effect tests in the past (Duriez et al., 2008; Steinbrück, 2009; Steinbrück and Bottcher, 2011; Perez-Feró et al., 2014; Perez-Feró et al., 2019). Based on those experiments the development of numerical models for severe accident codes was initiated (Bals et al., 2008; Beuzet et al., 2011; Bratfisch et al., 2013). The further developments and validation of codes, however, needed integral tests covering the typical phenomena in an air ingress scenario.

The first integral test with air ingress conducted in the CODEX facility (CODEX-AIT-1) was carried out in the framework of the EU OSPA project (Sheperd et al., 2000). The surprisingly intense oxidation in oxygen atmosphere led to temperature excursion already in the pre-oxidation phase in this first test. The second test (CODEX-AIT-2) was started with pre-oxidation in steam and the final air ingress was initiated

* Corresponding author.

E-mail address: robert.farkas@ek-cer.hu (R. Farkas).

later. The metallographic examination of CODEX-AIT-1 and CODEX-AIT-2 tests showed that oxides and nitrides formed not only in regular layers in the zirconium cladding, but also created complex microstructures (Hózer et al., 2003). Uranium containing aerosols were released – the pellets were made of depleted uranium-dioxide –, but the oxidation of UO_2 to higher oxides in high-temperature air was not detected (Csordás et al., 2000).

In the PARAMETER-SF4 test, moderate degree of pre-oxidation took place. During the air ingress phase the melting point of zirconium was reached at some elevations and molten materials filled part of the bundle cross section. The test was terminated by reflooding the bundle from the bottom. Nitrides were not identified in the post-test examinations (Stuckert et al., 2016).

In the QUENCH-10 experiment, high degree of pre-oxidation was reached (Schanz et al., 2006, Steinbrück et al., 2006). Due to low air flow rate, oxygen starvation took place in the upper part of the bundle that led to intense nitriding of the zirconium alloy cladding. During the reflood phase high nitrogen release was measured at the bundle outlet, that indicated the re-oxidation of part of the formed nitrides. In the QUENCH-16 test, also a low air flow was applied in the air ingress phase in order to create oxygen starvation conditions (Stuckert and Steinbrück, 2014). The final water quench led to significant temperature excursion, which was accompanied by high hydrogen and nitrogen release, indicating that both nitride re-oxidation and zirconium oxidation took place during reflood. QUENCH-18 was the first large-scale bundle test including a prototypical experiment stage in air + steam mixture (Stuckert et al., 2021). The temperature escalation during the air ingress was significantly stronger than for QUENCH-16 mainly due to additional exothermal cladding oxidation in steam. During the starvation period about 100 g oxygen and 450 g steam were consumed. During the steam consumption period about 45 g hydrogen were released. In the same time, a partial consumption of nitrogen (about 120 g) was registered. Formation of zirconium nitrides was observed in the bundle middle part. Initiation of reflood with 50 g/s water caused strong temperature escalation to about 2160 °C at the hottest bundle elevations resulting in about 238 g hydrogen release. This is significantly more than for QUENCH-16 (128 g) performed also under air ingress conditions, but with the formation of a smaller amount of melt. During re-oxidation of zirconium nitrides more than 54 g nitrogen and 15 g hydrogen were released.

BWR and PWR type fuel assemblies were tested at the Sandia National Laboratory in order to simulate the fuel degradation during loss of coolant accidents in spent fuel pools (Durbin and Lindgren, 2017; Lindgren et al., 2007; Lee and Kim, 2013). The tests were carried out in air atmosphere. After heating up the fuel rods, the exothermic zirconium reactions with air components started and the zirconium fire continued for several days. The temperature excursion was limited by the access of air to the bundles. In the first phase, the depletion of nitrogen in the outlet flow indicated that nitriding took place parallel with oxygen starvation. In the last phase, the zirconium-nitride was also re-oxidised. The tests ended with the complete oxidation of the zirconium

components.

The integral air ingress tests (Table 1) identified several important phenomena associated with the interaction between fuel rods and air. It could be concluded that chemical reactions are fast and intense in the presence of air and that several reactions can sometimes take place in parallel in the fuel bundles.

In the framework of the EU SAFEST project (Bechta et al., 2019; Miassoedov et al., 2015), it was proposed to carry out a new integral bundle test in which some parameters were not typical for reactor or spent fuel pool conditions, but the reactions between air and zirconium alloy were intentionally slowed down by controlling heating power and coolant flowrates. According to this approach, the individual phenomena could be better separated from each other and that would be an advantage for testing and developing numerical models. It was agreed that the reference scenario would be a reactor accident with melt through of bottom head and penetration of air from the reactor cavity into the reactor vessel. The degradation of the remaining fuel assemblies in the core periphery should take place in steam-argon mixture. Limited air and steam flow rates were intentionally selected in order to induce high-temperature chemical interactions under oxygen and steam starvation conditions. Slow cool-down was proposed to provide information on the state of the bundle before quench. The specification of test conditions was supported with pre-test calculations performed by EU SAFEST partners. The test bundle of the CODEX-AIT-3 experiment was a seven rod bundle simulating VVER fuel, while in the CODEX-AIT-1 and CODEX-AIT-2 experiments nine rod PWR type bundle was used. The pellets were made of UO_2 in the CODEX-AIT-1 and CODEX-AIT-2 experiments, but the CODEX-AIT-3 bundle had zirconia pellets. The objectives of the test was completely different. The oxidation of UO_2 and the temperature escalation in air was addressed in the CODEX-AIT-1 and CODEX-AIT-2 tests. The CODEX-AIT-3 test focused on the simulation of chemical reactions between air and zirconium, including oxygen starvation.

2. Test facility

The test facility included a bundle design, which is representative for VVER reactors with hexagonal arrangement of 7 rods. A schematic view of the facility is shown in Fig. 1. The basic part of the facility was the test section comprising the bundle. The bottom of the test section was connected to the steam generator unit. The condenser cooled down the hot steam + gas flowing out from the top of the test section.

The fuel bundle consisted of six electrically heated fuel rods of 1000 mm length in the periphery and one unheated rod in the centre (Fig. 2). The cladding material was Russian sponge based E110 alloy. The external diameter of the cladding was 9.1 mm. ZrO_2 pellets with 7.65 mm diameter were used inside of the rod and 9.0 mm diameter pellets were applied in the bottom connections of the rod.

The six peripheral rods were heated and not pressurized. Electrical heating with two tungsten heaters (0.049 Ω/m) in each rod was applied. ZrO_2 ceramic pellets were used. The heated length was 990 mm, the total length of the rod was 1000 mm.

The central rod was not heated, but it was pressurized during the test in order to reach ballooning and burst in the early phase of the experiment. The central rod was also filled with ZrO_2 pellets.

The rods in the bundle were fixed by three spacer grids made of Zr1% Nb alloy. The bundle was placed into a hexagonal shroud. The shroud material was Zr2.5 %Nb alloy (Table 2). The inlet junction was located at 20 mm and the outlet junction at 1020 mm elevation (0 mm corresponds to the bottom of bundle). The upper head of the test section was cooled by a water loop. The bundle was heated by DC power supply units.

The shroud had no perforations and it was surrounded by several thermal insulation layers, electrical heaters and a steel tube (Fig. 2). $SiO_2 + Al_2O_3 + ZrO_2$ fibre was used between the Zr shroud and the steel tube.

Table 1
Integral air ingress tests with electrically heated bundles.

Test	Bundle type	Year
CODEX-AIT-1	PWR 3 × 3 bundle with UO_2 pellets	1998
CODEX-AIT-2	PWR 3 × 3 bundle with UO_2 pellets	1999
PARAMETER-SF-4	19-rod VVER bundle with UO_2 pellets	2009
QUENCH-10	21-rod PWR bundle with ZrO_2 pellets	2004
QUENCH-16	21-rod PWR bundle with ZrO_2 pellets	2011
QUENCH-18	24-rod PWR bundle test with ZrO_2 pellets and two absorber rods	2021
Sandia BWR fuel tests	Full and partial length 9 × 9 BWR assemblies with MgO pellets	2004–2006
Sandia PWR fuel tests	Full scale 17 × 17 PWR assemblies with MgO pellets	2011–2012

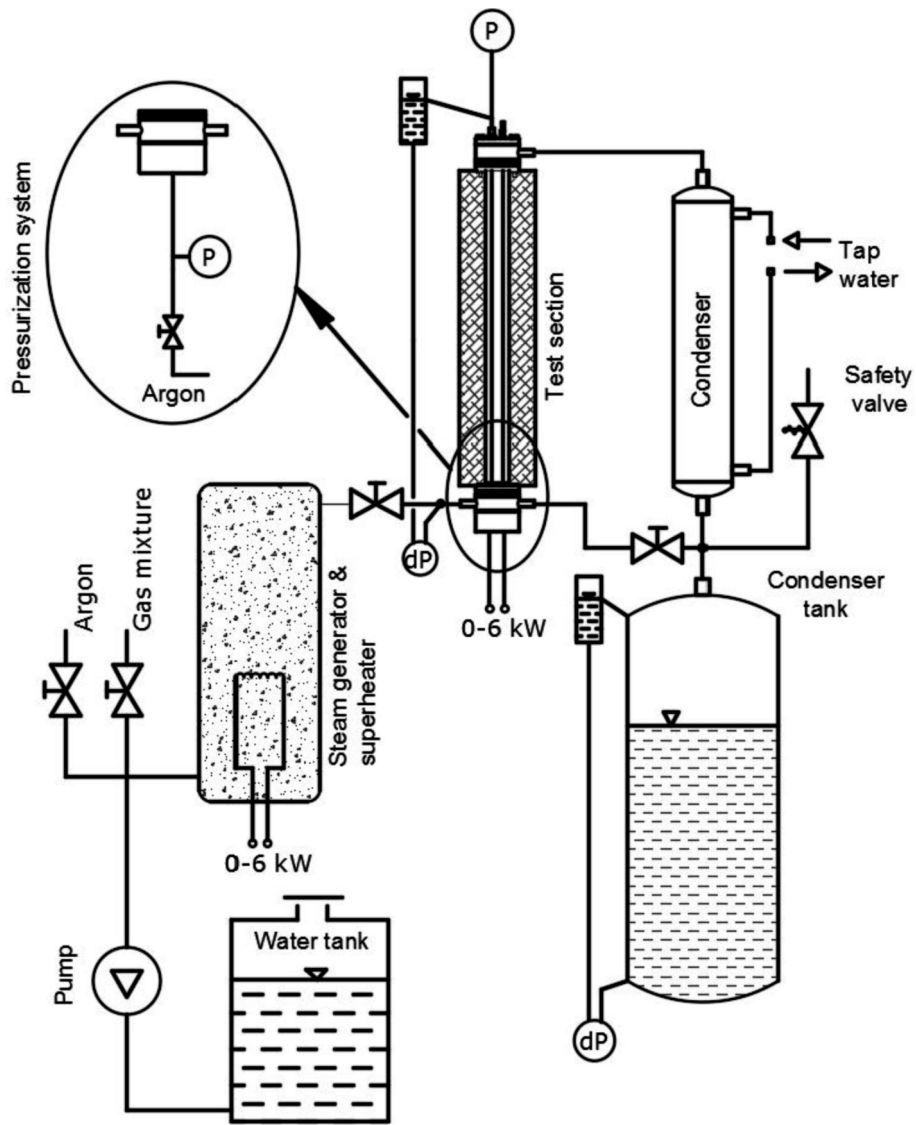


Fig. 1. Schematic view of the CODEX facility.

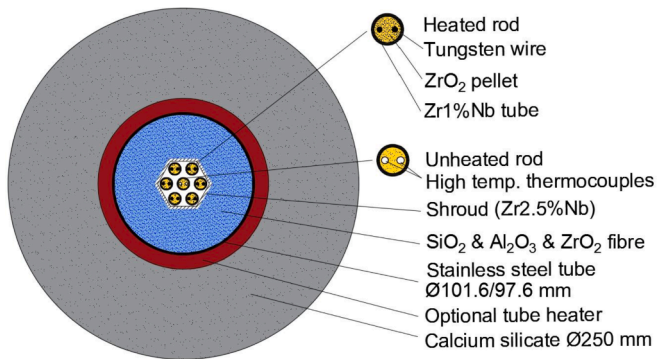


Fig. 2. Cross section of the test section with thermal insulations.

Steel vessel (diameter 101.6/97.6 mm) with external electrical heating housed the test section with fibre insulation. External heaters were applied on the surface of the stainless steel tube.

Calcium silicate covered the steel tube as external layer of thermal insulation with external diameter of 250 mm.

The steam generator provided hot steam to the test section during the

Table 2

Main characteristics of the test section.

Number of fuel rods	7
Cladding alloy	sponge based E110
Length of fuel rods	1000 mm
External diameter of fuel rods	9.1 mm
Cladding wall thickness	0.69 mm
Pellet material	ZrO ₂
Height of pellet	10 mm
Diameter of pellet	7.65 mm
Hole diameter in the pellet	2 mm
Spacer grid material	Zr1%Nb
Height of spacer grid	10 mm
Thickness of spacer grid	0.4 mm
Number of spacer grids	3
Shroud material	Zr2.5 %Nb
Shroud thickness	2 mm
Shroud key size	39 mm

pre-oxidation phase of the test. The water injection into the steam generator was performed with an OBL type precision pump at constant flow rate. For heating up, cold argon gas at a high flow rate was also injected into the steam generator.

During the air oxidation phase of the test, a small amount of water was injected onto the bottom of the bundle using an HPLC pump (Liquopump 312/1). Low flow rate argon and air was injected also directly to the bottom of the bundle through a heated line.

On-line gas composition measurement at the test section outlet was performed by a quadrupole mass spectrometer (OmniStar GSD 320 O2). All gas lines (sampling tube, valve, capillary inlet of the mass spectrometer) were heated to about 150 °C, which allowed the measurement of the steam concentration in the outlet gas. Besides steam, concentrations of hydrogen, oxygen, nitrogen, and argon in the off-gas were measured during all test phases.

3. Single rod test

A single-rod heating test was carried out before the bundle test to check the operability of the facility. The temperature went beyond 1000 °C (Fig. 3) and the thermal conditions could be kept for more than one hour. Degradation was observed in the lower part of the rod. It was suspected that eutectic interactions took place between the non-oxidized cladding surface and the K type thermocouple.

In the second single-rod test again strong degradation was found in the lower part of the rod. The thermocouple this time was insulated, so the eutectic interaction could not be the cause. It was concluded that the high voltage (30 V) AC power could result in partial shortcut in the lower section of the rod and it could lead to degradations shown in Fig. 4.

The solution for this two-wire heating approach was the use of DC power which has lower voltage at the same power compared to AC. For this reason, the CODEX power supply system was redesigned and rebuilt. DC power was applied in the integral CODEX-AIT-3 test.

4. The CODEX-AIT-3 experiment

The CODEX-AIT-3 experiment test started with several technological actions.

The experiment included five main phases.

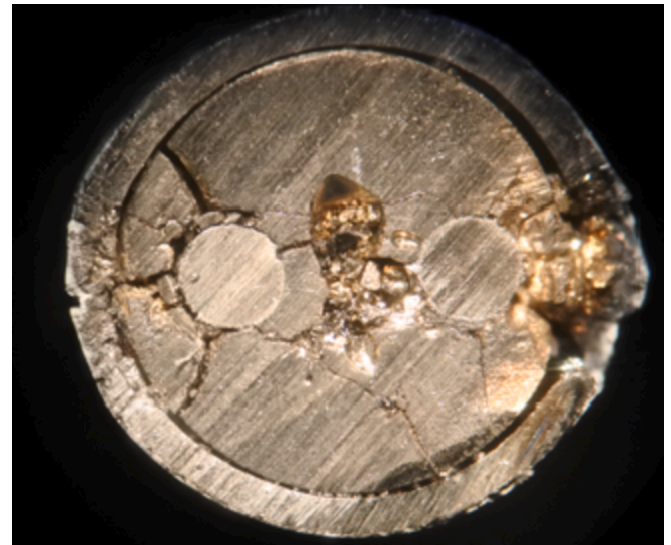


Fig. 4. Cross section of the degraded bottom part of the second single rod.

4.1. Heat-up phase

Technological heat-up phase started with switching on the external heaters with 750 W power. The argon flow rate in the gap between shroud and stainless steel tube was set to 0.15 g/s. The argon and steam flows through the bundle were initiated with 0.12 g/s and 1.0 g/s flow rates, respectively. The water cooling system was put into operation; the bundle power was set to 500 W and later to 600 W. Meanwhile the argon flow rate (to the bundle) was set from 0.12 g/s to 1.0 g/s (Fig. 5). A pressure test was performed on rod No. 1, the maximum value reached 33.7 bar.

4.2. Pre-oxidation phase

The pre-oxidation phase was initiated after 6800 s. The bundle

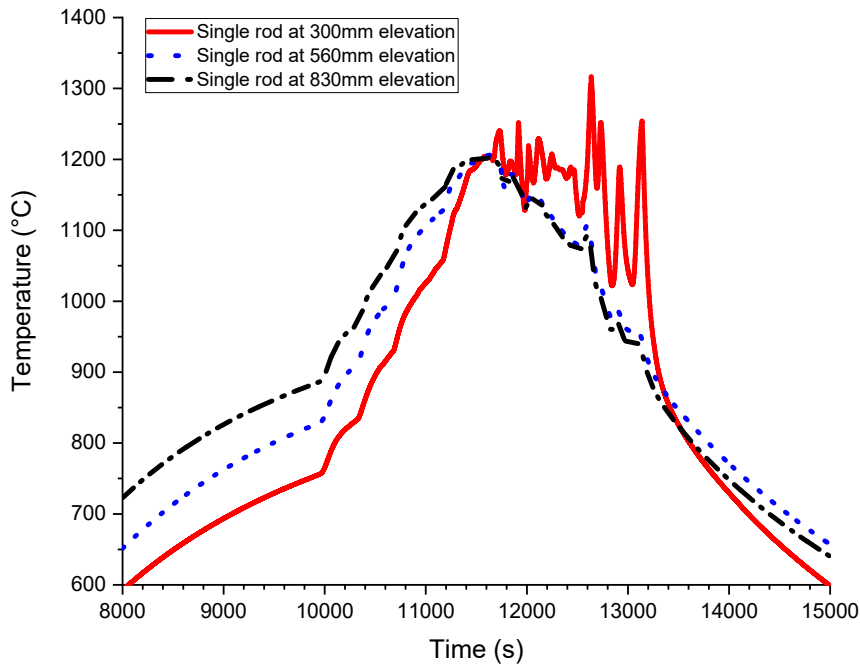


Fig. 3. Cladding temperatures during the first single rod experiment.

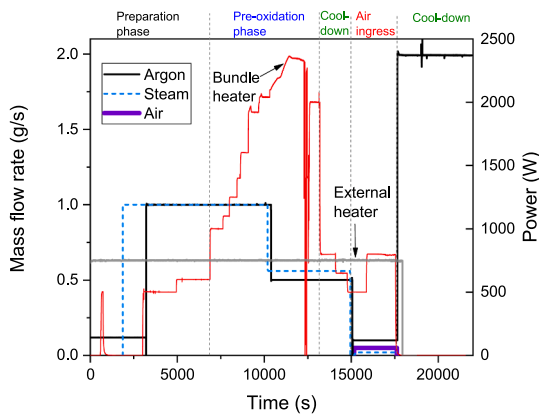


Fig. 5. Power, steam and gas flow rates history during the CODEX-AIT-3 test.

power was increased in a stepwise manner up to 1920 W. The power increase resulted in significant heat-up of the bundle. When the temperature at 850 mm elevation was about 840 °C (9400 s), the central rod was pressurised and the burst took place at 67.2 bar (Fig. 6). Both steam and argon flow rates were reduced from 1.0 g/s to 0.5 g/s after 10000 s in order to reach higher temperature increase for the bundle. The maximum temperature reached at 750 mm elevation was 1150 °C at 12300 s. In order to avoid a too high degree of oxidation in this phase, the high temperature plateau was maintained for 15 min by manipulating the bundle power. The maximum electric power of the bundle was 2500 W. At the end of the pre-oxidation phase, the rod maximum temperature was 1160 °C, while the shroud heated up to 1135 °C and the stainless steel tube temperature was above 750 °C. During the pre-oxidation phase, the axial temperature profiles had a maximum at the top of the bundle. The total hydrogen release measured in the pre-oxidation phase was about 3.8 g. The hydrogen generation data were in good accordance with the measured temperatures of the rods.

4.3. Intermediate cool-down phase

An intermediate cool-down phase was started with power reduction after 13000 s and the steam generator was switched off. The maximum rod temperature decreased to 925 °C (Fig. 7).

4.4. Air-ingress phase

The air-ingress phase started after 15000 s. The argon flow rate was reduced from 0.5 g/s to 0.1 g/s and the air flow was initiated with 0.05 g/s flow rate. 0.02 g/s water injection to the bottom of the bundle was initiated supplied by a small pump. The bundle power was increased to 800 W. The temperature of 1000 °C was reached at 750 mm elevation after 16150 s. Due to the low flow rates, both steam and oxygen starvation was established in the upper part of the bundle and the chemical reactions became most intense in the less oxidised middle and lower parts of the bundle. The maximum measured temperature was 1625 °C recorded at 300 mm elevation. During the air-ingress phase, the maximum temperatures moved to the centre of the bundle (Fig. 8). After beginning of air ingress, first oxygen was completely consumed from the gas stream through the bundle at about 16750 s (Fig. 9). From that time, considerable nitrogen consumption started, which indicates that global oxygen and steam starvation was established at the upper part of the bundle. Parallel with oxygen, steam was also consumed from the beginning of the air-ingress phase and shortly after the complete oxygen consumption, it was also fully consumed at about 17200 s. Despite the detected steam consumption from the start of the air-ingress phase, hydrogen produced by the zirconium-steam reaction became detectable in the outlet gas only after the complete consumption of oxygen. As long as oxygen was available, the evolving hydrogen recombined with oxygen and produced water. There was complete oxygen and steam starvation in the upper part of the bundle for about 7 min. The onset of this phase coincides with the temperature escalation of the lower-middle part of the bundle (at 300–500 mm). From about 17400 s, the quantity of nitrogen started to increase in the outlet gas due to the re-oxidation of the formed nitrides. The total hydrogen release measured

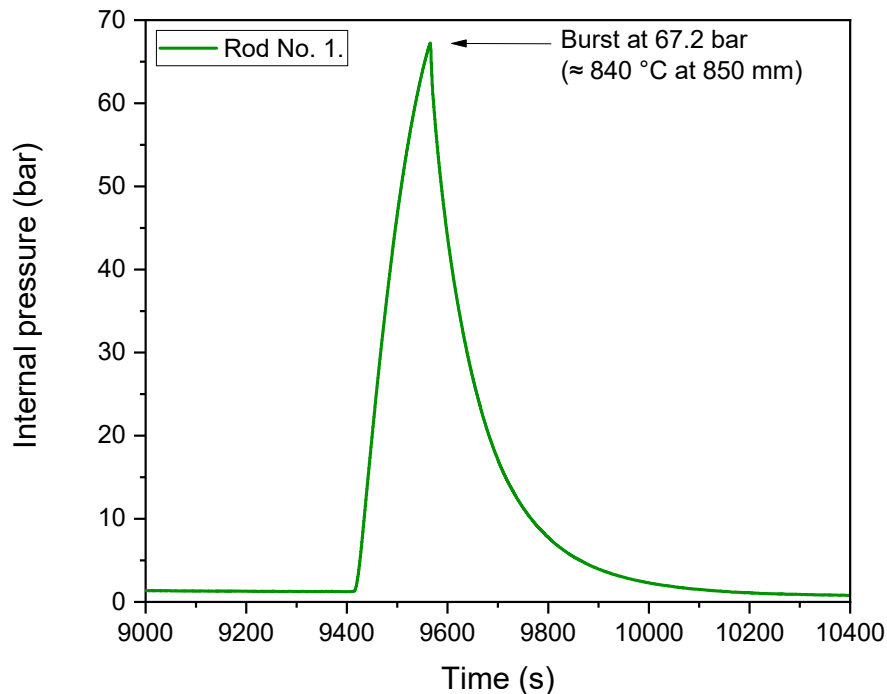


Fig. 6. Internal pressure in central unheated rod (rod No. 1).

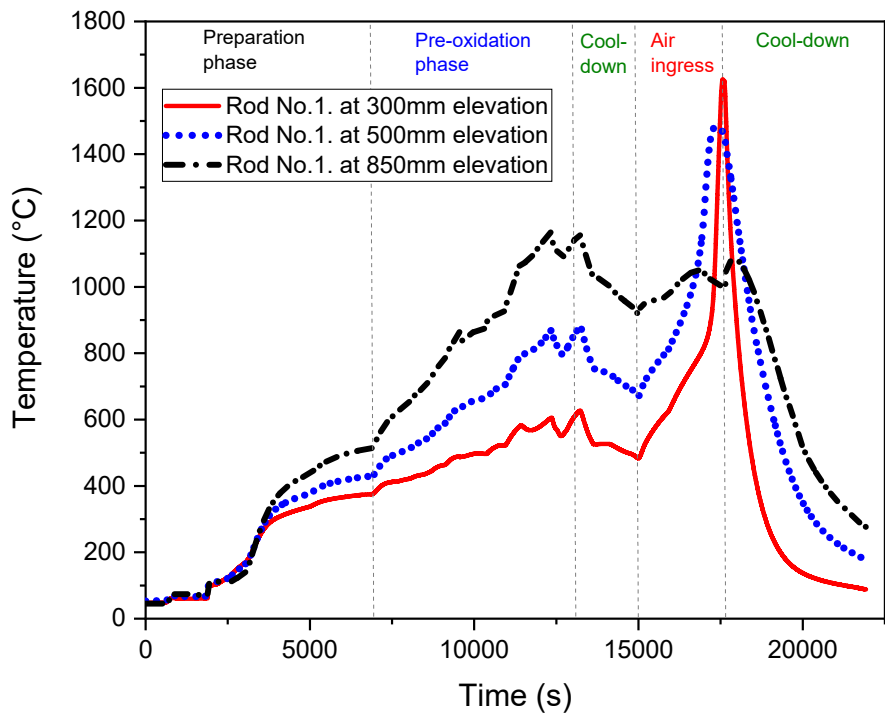


Fig. 7. Fuel rod No. 1. temperatures.

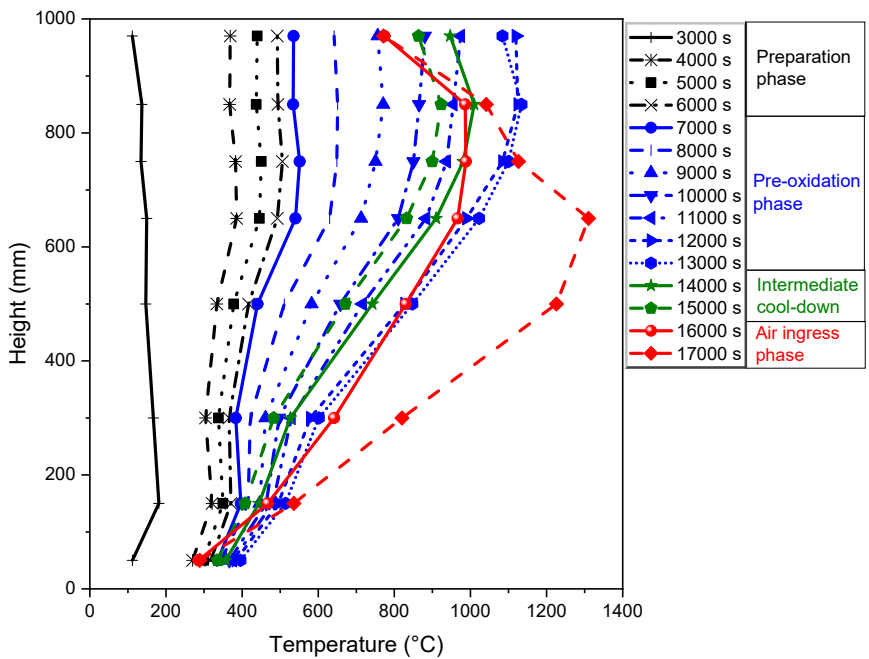


Fig. 8. Axial temperature profiles of the bundle using the maximum local temperatures.

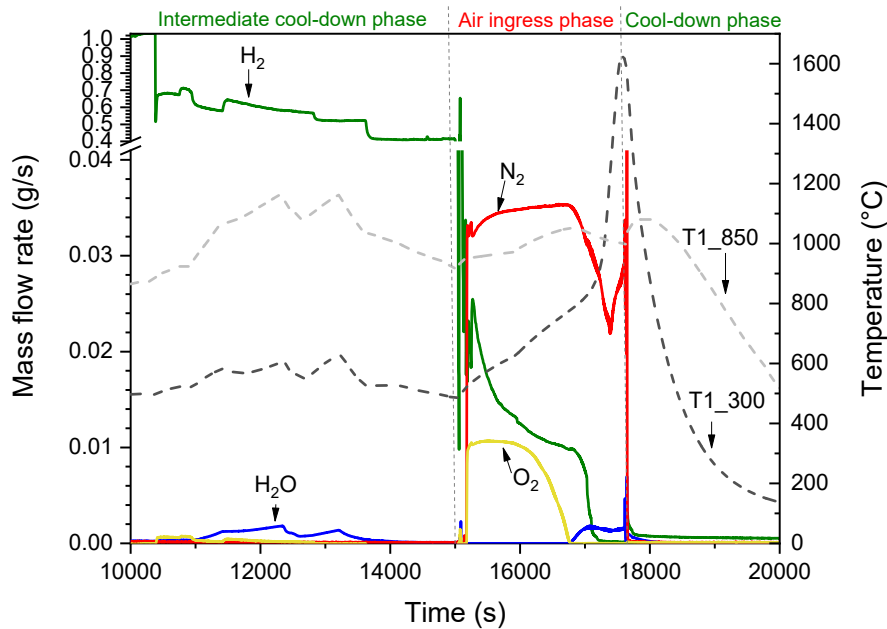


Fig. 9. Measured gas flow rates and fuel rod No. 1 temperatures (at elevation 300 and 850 mm) in the pre-oxidation and air-ingress phase of the CODEX-AIT-3 experiment.

in the air-ingress phase was about 1.4 g, while the total uptake of oxygen and nitrogen was about 12 and 13 g, respectively.

4.5. Cool-down phase

Final slow cool-down was applied with switching off the bundle and external heater power. The steam and air flow rates were set to zero, while the argon flow rate was increased to 2.0 g/s. It took more than two hours to cool-down the facility and after that, the water cooling system was switched off.

5. Main results of on-line measurements

The CODEX-AIT-3 experiment was a rather complex test with sophisticated boundary conditions. The experiment was carried out under conditions, which were close to the specified ones by pre-test calculations.

The main targets of the test were reached:

- Cladding burst took place at 840 °C due to pressurization of the central rod. The opening allowed the coolant to enter into the rod and start chemical reactions on both sides of the cladding.
- Pre-oxidation was carried out in high flow rate steam with maximum temperature above 1100 °C. The estimated oxide scale thickness in the hottest section of the bundle reached 100 μm.
- During the intermediate cool-down phase the temperatures were reduced to below 925 °C.
- The duration of the air ingress phase was 1 h, and the maximum cladding temperature was slightly above 1600 °C.
- The outlet gas composition showed that during the air ingress phase, steam and oxygen starvation conditions were established. The partial consumption of nitrogen also indicated the formation of nitrides.
- The temperature profile significantly changed during the air ingress phase: the maximum temperature moved from the upper section to the middle part of the bundle due to the intense chemical interactions in the less oxidised central part.
- Cool-down of the bundle was performed in argon in order to avoid interactions that might have taken place during water quench.

6. Post-test examination results

After the experiment, the bundle was removed from the test section and the degraded structure was fixed by epoxy. 17 cross sections were prepared for further examinations at the following elevations:

200, 250, 300, 350, 400, 450, 500, 550, 600, 650, 700, 750, 800, 850, 900, 950 and 1000 mm.

Cladding burst was observed on the central rod at 900 mm elevation (Fig. 10).

The detailed examination of cross sections by optical microscopy provided the following results:

- At 300 mm elevation, the central rod was oxidised on both sides, and nitrides could be observed in different positions both inside and outside of the oxide layer. The oxide scale on rod No. 5. was about

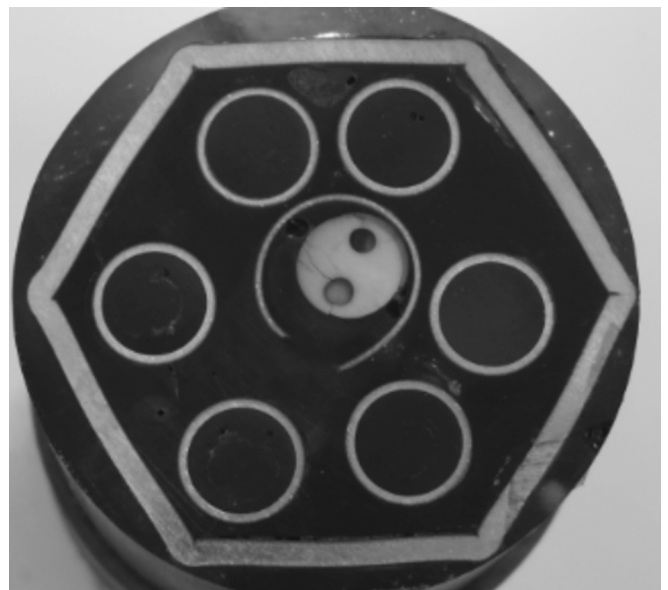


Fig. 10. Cross section of the CODEX-AIT-3 bundle at 900 mm elevation.

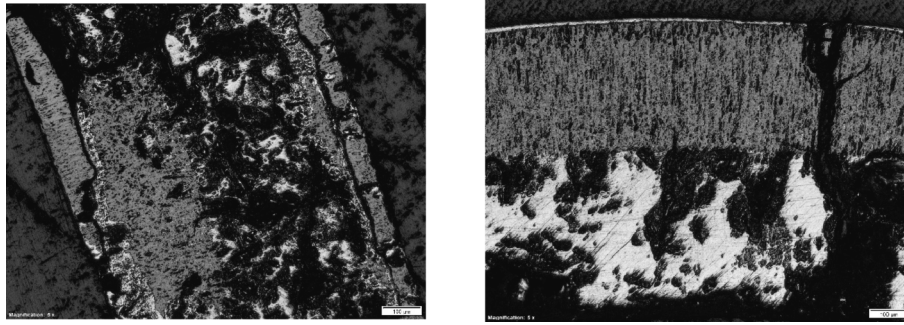


Fig. 11. Optical microscopy pictures of rod No. 1. (left) and No. 5. (right) at 300 mm.

300 μm thick and a thin nitride layer was formed on its external surface (Fig. 11).

- At 400 mm elevation, cracked oxide scale can be seen on the central rod with several small nitrified regions. In spite of the fact that the burst took place at the top of the bundle, the internal oxidation and nitriding was significant even at low elevations (300 and 400 mm). Rod No. 2. was also oxidised and nitrified. The oxide scale thickness was about 100 μm (Fig. 12).
- At 550 mm elevation, both central and peripheral (No. 7.) rods were covered by significant amount of nitrides. This structure indicated that oxygen starvation took place at this elevation in the last phase of the test. The presence of nitrides at the oxide- α layer interface shows that this part was strongly affected by air oxidation before global oxygen starvation took place due to local oxygen starvation in this region (Fig. 13).
- At 650 mm, the regular structure of oxide and nitride on the external surface of the central rod suggests that the oxide was formed in steam and the nitriding process happened in oxygen starving conditions. Similar conclusions can be drawn based from the oxide structure of rod No. 3: the cracked oxide layer is covered by nitrides on all its free surfaces (Fig. 14).
- At 750 mm elevation, the nitrides were formed mainly at the inner side of the oxide layer and interesting (arc-like) structures were formed. A small amount of nitride formation is also observed on the outer surface of the oxide layer. Probably the temperature in the last phase of the experiment was not high enough at this elevation to initiate intense chemical reaction between Zr and nitrogen (Fig. 15).
- At 900 mm, the opening at the burst position was oxidised on both sides. The oxide scale on rod No. 2 did not reach 100 μm . Nitrides were not formed at this elevation due to quite low temperatures during air ingress (Fig. 16).

The observations carried out confirm the phenomenology of the processes of nitride formation, previously studied in detail in single-effect tests. Namely, nitrogen reacts with areas of $\alpha\text{-Zr(O)}$ (Steinbrück, 2014, Grosse et al. 2016, Grosse et al. 2018). Such areas are formed

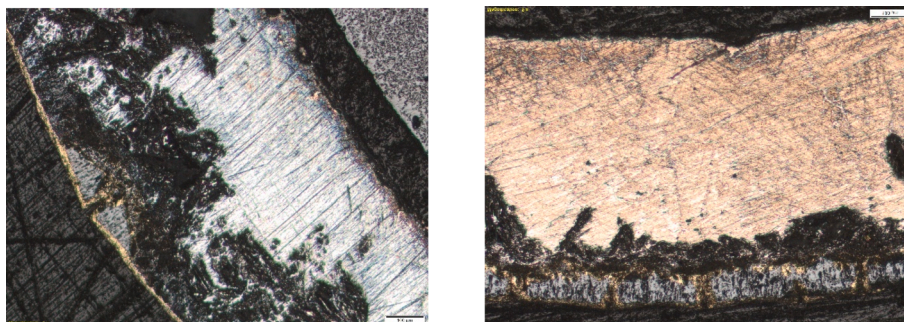


Fig. 12. Optical microscopy pictures of rod No. 1. (left) and No. 2. (right) at 400 mm.

during the stage of oxygen starvation both on the outer surface of the oxide layer and in its bulk (Stuckert and Veshchunov, 2008).

The examinations included the determination of layer thicknesses on the cladding tubes and shroud. The following layers were measured in those cross sections where they could be identified:

- oxide layer on the external surface of cladding tubes,
- oxide layer on the internal surface of cladding tubes,
- oxide layer on the external surface of shroud,
- oxide layer on the internal surface shroud,
- $\alpha\text{-Zr(O)}$ layer,
- nitride layer on the external surface of oxide,
- nitride layer at the $\alpha\text{-Zr(O)} - \text{ZrO}_2$ interface.

The layer thicknesses were measured at several positions on each fuel rod in a given elevation. The scatter of measured data in some cases was very significant, which indicates that heterogeneous microstructures were produced. Especially the nitrides showed complex structures, like small spots, islands and arcs, but compact nitride segments were produced as well.

Based on the above-described typical structures, the following layer thicknesses were measured where they were available (Fig. 17):

- $\text{ZrN}^{\text{ex}}_{\text{out}}$ – nitride layer on the external surface of the outer oxide scale.
- transition layer – layer between external nitride layer and outer oxide layer.
- $\text{ZrO}_2_{\text{out}}$ – oxide layer on the outer surface of the cladding.
- $\text{ZrN}^{\text{met}}_{\text{out}}$ – nitride layer on the metallic surface on the outer side of cladding.
- $\alpha(\text{O})_{\text{out}}$ – alpha layer on the outer side of the cladding.
- ZrO_2_{in} – oxide layer on the inner surface of the cladding.

6.1. Oxide layer thickness on fuel rods

The oxide layer thickness for each fuel rod was measured at each cross section in several positions.

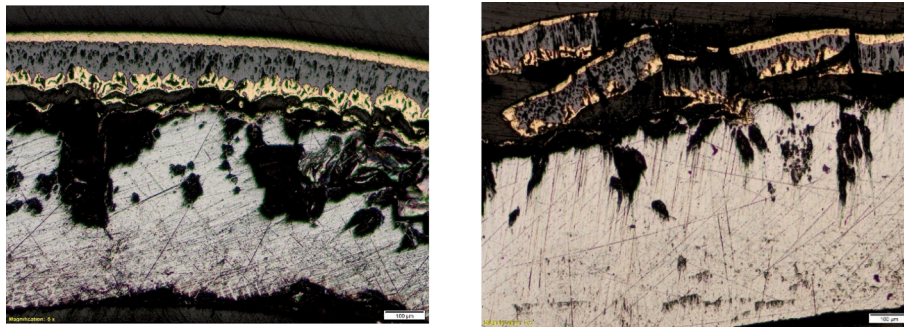


Fig. 13. Optical microscopy pictures of rod No. 1. (left) and No. 7. (right) at 550 mm.

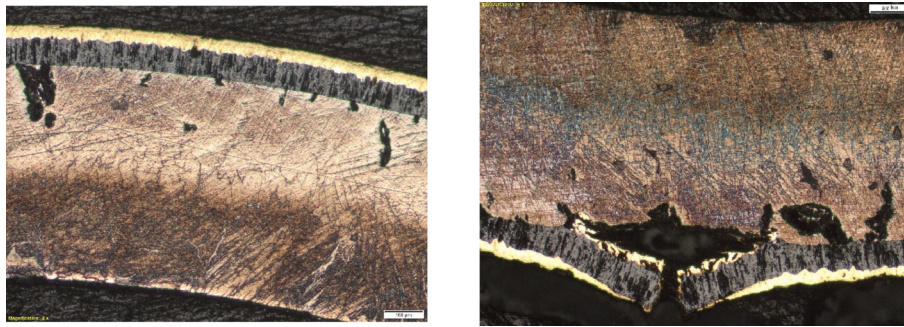


Fig. 14. Optical microscopy pictures of rod No. 1. (left) and No. 3. (right) at 650 mm.

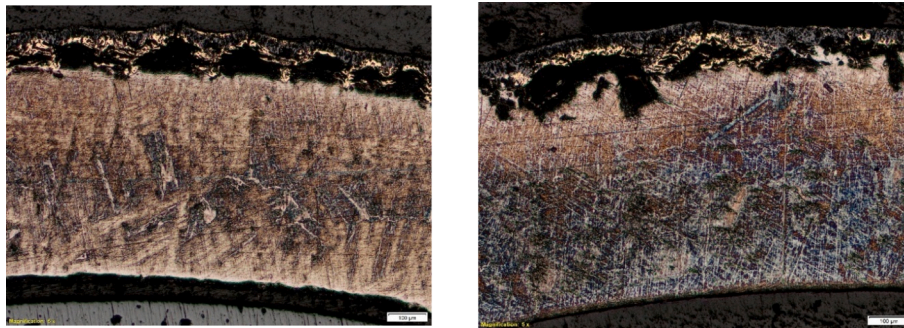


Fig. 15. Optical microscopy pictures of rod No. 1. (left) and No. 4. (right) at 750 mm.

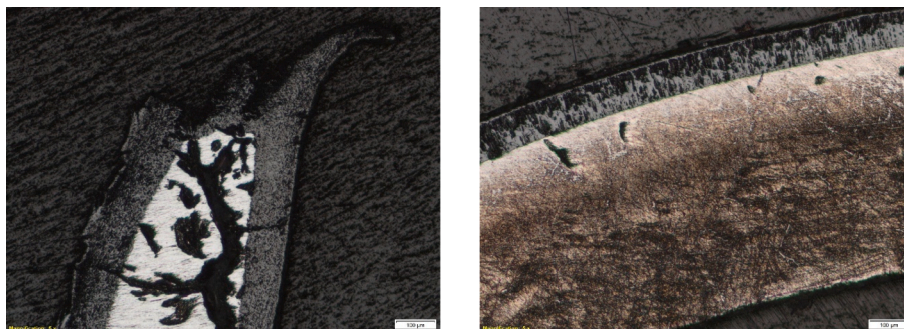


Fig. 16. Optical microscopy picture of rod No. 1. (left) and No. 2. (right) at 900 mm.

The average values of oxide layer thickness on the outer surface of the fuel rods are summarised in Fig. 18. The maximum oxide thickness close to $300\ \mu\text{m}$ was measured at 300 mm elevation. In the upper part of the bundle, the typical oxide thicknesses were around $100\ \mu\text{m}$. The differences in the oxide layer thickness (e.g. at 300 mm) on the rods

were probably related to the variation of radial temperature profile. However, it could not be evaluated numerically, since there was only one thermocouple at that elevation.

Oxide layer on the inner surface of the cladding tubes was observed only at some selected positions. The fuel rod No. 5. and No. 3. showed

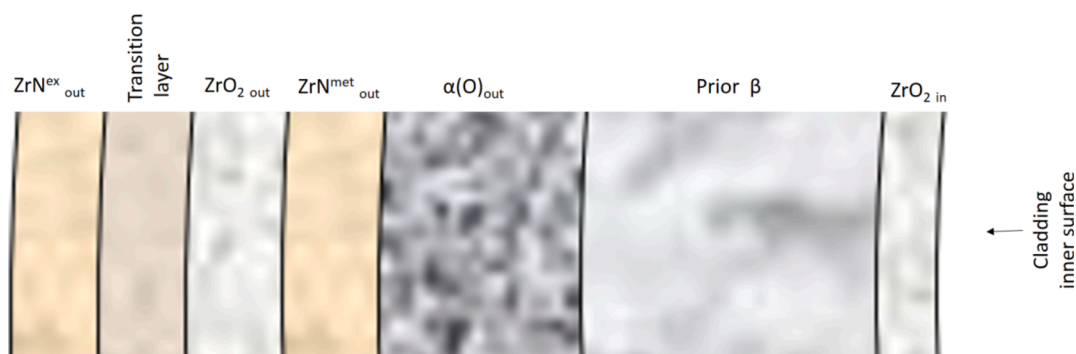


Fig. 17. Layers identified on cladding tube cross sections.

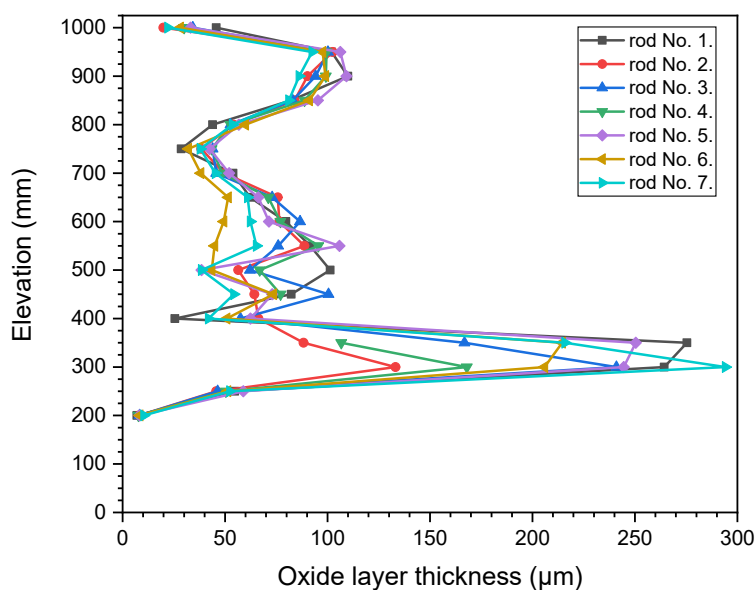


Fig. 18. Oxide layer thickness on the outer surface of fuel rods.

slight oxidation on part of their inner surfaces at 350 mm and 450 mm elevations, respectively. Some cracks were seen on the cladding tubes at those locations, so probably the brittle failure of the fuel rods allowed the penetration of the coolant. The central rod (No. 1.) of the bundle was damaged during the experiment due to ballooning and burst, and oxidation of the inner surface took place between 850 and 950 mm elevation, the average value of oxide scale was 70–80 μm.

6.2. Nitride layer thickness on fuel rods

Nitride layer thickness for each fuel rod was measured at each cross section at several positions, where such layers were formed. The nitride layer on the external surface was observed between 250 and 850 mm elevations, while the nitride layer at the metal/oxide interphase was seen between 400 and 750 mm. The total nitride layer thickness on the outer surface of the cladding was calculated as the sum of two individual layers.

The measured data showed heavy nitriding at 450–700 mm elevations (Fig. 19), where the maximum values of total thickness nitride layers reached 100 μm.

6.3. α -Zr(O,N) layer thickness on fuel rods

Since oxidation of the cladding tubes was mainly limited to the outer surface, the oxygen-rich α -Zr(O) layers were formed only at the outer cladding surface. Significant α layer thickness was measured above 500 mm elevation, where the oxidation of cladding was not as extensive as around 300 mm. The α -Zr(O) layer thickness reached 200–300 μm.

6.4. Transition layer thickness on fuel rods

A transition layer between nitride and oxide layers was found in several positions between 300 and 600 mm elevations. The average value of transition layer thickness was around 20 μm.

6.5. Measurements on the shroud

The shroud cross sections showed even more complex structure than that of cladding tubes. Nitride layers were found on both inner and outer surfaces and the oxide on the inner surface in some positions was divided into two separate layers by the external nitride layer. The general structure of the shroud is composed by the following layers (Fig. 20):

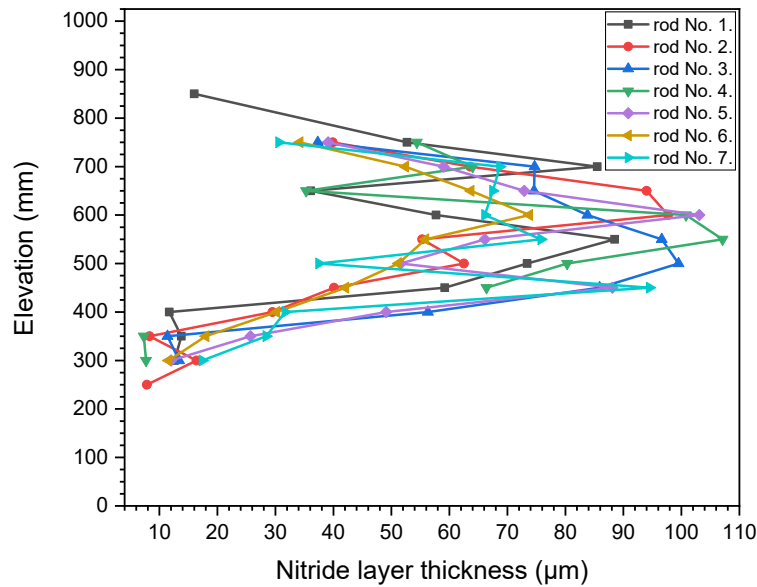


Fig. 19. Total thickness of nitride layers on fuel rods.



Fig. 20. Layers identified on shroud cross sections.

- $ZrO_2^{ex}_{in}$ – oxide layer on the inner surface of the shroud.
- ZrN^{ex}_{in} – nitride layer on the external surface of the inner oxide scale.
- transition layer – layer between external nitride layer and inner oxide layer on the metallic surface.
- $ZrO_2^{met}_{in}$ – oxide layer on the inner surface of the shroud close to the metallic surface.
- ZrN^{met}_{in} – nitride layer on the metallic surface on the inner side of shroud.
- $\alpha(O)_{in}$ – alpha layer on the inner side of the shroud.
- $\alpha(O)_{out}$ – alpha layer on the outer side of the shroud.
- ZrN^{met}_{out} – nitride layer on the metallic surface on the outer side of shroud.
- ZrO_2^{out} – oxide layer on the outer surface of the shroud.
- ZrN^{ex}_{out} – nitride layer on the external surface of the outer oxide scale.

The maximum oxide layer thickness on the inner surface of the shroud was observed at 200 mm elevation. The axial profile of oxide layers on the cladding outer surface (Fig. 18) and on the shroud inner surface (Fig. 21) are similar.

Similar profiles of nitride layers on the cladding outer surface (Fig. 19) and on the shroud inner surface (Fig. 22) could be also seen with maximum values between 400 and 700 mm.

The α -Zr(O) layers were found close to both inner and outer surfaces on the shroud above 500 mm elevation.

7. Conclusions

The CODEX-AIT-3 experiment demonstrated several phenomena that may be expected in a nuclear reactor severe accident with air ingress. The fuel bundle was heated up to 1600 °C to allow high-temperature interactions. The air ingress phase lasted for one hour. The steam and air flow rates were regulated in such a way that starvation conditions were obtained in some locations of the bundle.

Different chemical interactions were identified by the on-line measurements and post-test examinations.

- The presence of hydrogen in the outlet gas composition showed that steam oxidation of zirconium took place. Part of the oxide observed in the metallography analyses was produced by steam and another part by the oxygen from air.
- The reduction of nitrogen concentration in the outlet gas indicated that nitriding also took place. Furthermore, the later increase of nitrogen concentration indicated that re-oxidation of nitrides also happened, when steam was available again.

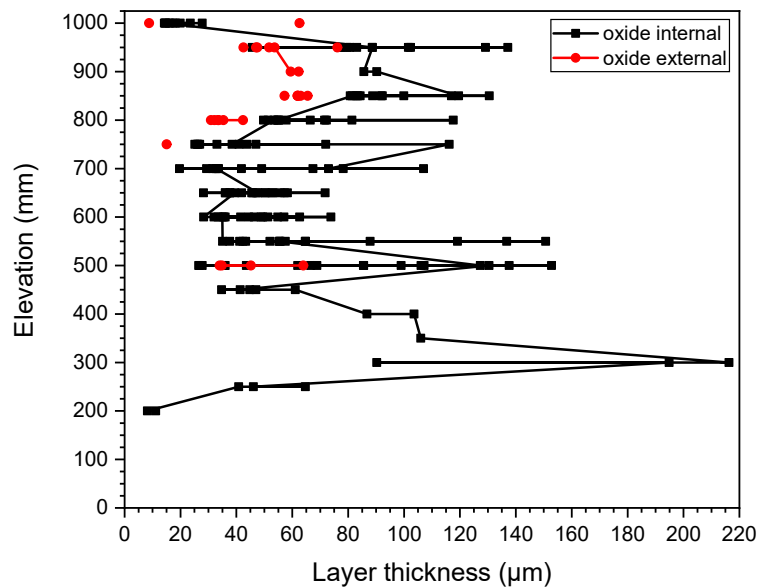


Fig. 21. Oxide layer thicknesses on shroud.

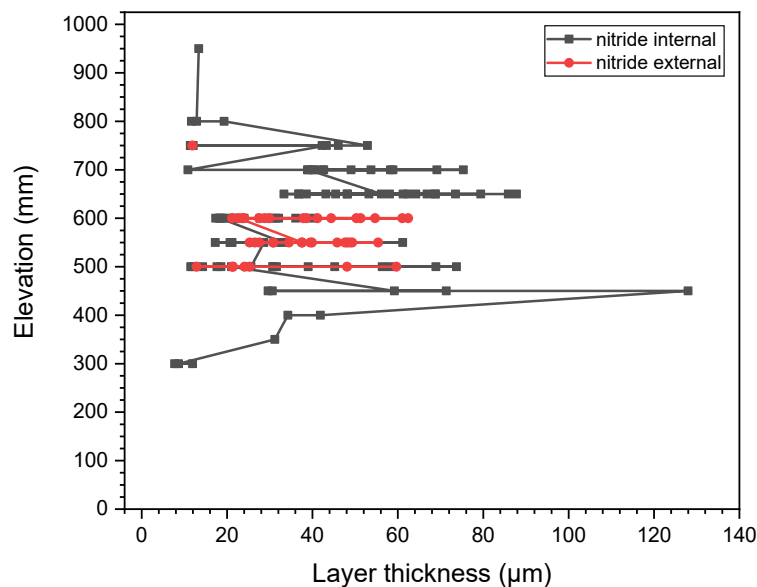


Fig. 22. Nitride layer thicknesses on shroud.

The microstructure of the cladding tubes showed a large variety along the length of the bundle. In a simplified way, seven layers could be identified in the cladding (external nitride, transition layer, external oxide, inner nitride, α -Zr(O), prior β -Zr and inner oxide). However, these layers were not regular. Some of these layers were missing in some positions. In other parts, incursion of different phases into each other through peninsula or island like segments could be detected. The microstructure of the zirconium shroud was even more complex, because both sides of the shroud were accessible for the coolant.

The local intensity of chemical reactions resulted in significant changes in the temperature profile. The maximum temperatures first were assigned to the top of the bundle. Later, due to limited steam and oxygen supply, the maximum temperature moved down to the positions, where still active oxidation took place.

The CODEX-AIT-3 experiment well illustrated the complex reactions that can take place in air ingress accident scenarios resulting in manifold microstructures. The results of this semi-integral bundle test well correlate with separate-effects studies conducted in the past.

The previous air ingress bundle tests were generally characterised by very intense interactions between air and zirconium. In the CODEX-AIT-3 test limited air and steam flow rates were selected, which slowed down the high temperature chemical interactions and provided unique data on nuclear fuel behaviour under oxygen and steam starvation conditions. The individual oxidation and nitriding phenomena were well separated from each other as it was indicated by the microstructure of zirconium components. This separation was observed in both time and location. Since the competition between different chemical reactions could be excluded in some locations and some time periods, the post-test numerical analyses of the experiment could be used for the evaluation of the role of numerical models developed for individual chemical reactions in severe accident codes.

Funding

The CODEX-AIT-3 experiment was supported by the EU 7th Framework Programme under Agreement n° 604771 (EU SAFEST project).

CRedit authorship contribution statement

Róbert Farkas: Methodology, Investigation, Visualization. **Zoltán Hózer:** Conceptualization, Supervision. **Imre Nagy:** Methodology, Investigation. **Nóra Vér:** Investigation. **Márta Horváth:** Investigation. **Martin Steinbrück:** Conceptualization. **Juri Stuckert:** Conceptualization. **Mirco Grosse:** Conceptualization.

Declaration of Competing Interest

The authors declare that they have no known competing financial interests or personal relationships that could have appeared to influence the work reported in this paper.

Acknowledgements

The authors are grateful to Thorsten Hollands (GRS), Leticia Fernandez Moguel (PSI), Yazan Alatrash (JAEC), Alexander D. Vasiliev (IBRAE) and Pál Kostka (NUBIKI) for executing valuable pre-test and post-test calculations.

References

- Adroguer, B., Bertrand, F., Chatelard, P., Cocuau, N., Van Dorsselaere, J.P., Bellenfant, L., Knocke, D., Bottomley, D., Vrtlikova, V., Belovsky, L., Mueller, K., Hering, W., Homann, C., Krauss, W., Miassoedov, A., Schanz, G., Steinbrück, M., Stuckert, J., Hózer, Z., Bandini, G., Birchley, J., Berlepsch, T.v., Kleinhietpass, I., Buck, M., Benitez, J.A.F., Virtanen, E., Marguet, S., Azarian, G., Caillaux, A., Plank, H., Boldyrev, A., Veshchunov, M., Kobzar, V., Zvonarev, Y., Goryachev, A., 2005. Core loss during a severe accident (COLOSS). *Nucl. Eng. Des.* 235 (2-4), 173–198.
- Auvinen, A., Brillant, G., Davidovich, N., Dickson, R., Ducros, G., Dutheillet, Y., Giordano, P., Kunstar, M., Karkela, T., Mladin, M., Pontillon, Y., Seropian, C., Vér, N., 2008. Progress on ruthenium release and transport under air ingress conditions. *Nucl. Eng. Des.* 238 (12), 3418–3428.
- Bals, C., Beuzet, E., Birchley, J., Coindreau, O., Ederli, S., Haste, T., Hollands, T., Koch, M. K., Lamy, J.-S., Trambauer, K. (2008). Modelling of accelerated cladding degradation in air for severe accident codes. In *Proceedings 3rd European Review Meeting on Severe Accident Research (ERMSAR 2008)*, Nessebar, Bulgaria (pp. 23–25).
- Bechta, S., Ma, W., Miassoedov, A., Journeau, C., Okamoto, K., Manara, D., Bottomley, D., Kurata, M., Sehgal, B.R., Stuckert, J., Steinbrück, M., Fluhrer, B., Keim, T., Fischer, M., Langrock, G., Piluso, P., Hózer, Z., Kiselova, M., Belloni, F., Schyns, M., 2019. On the EU-Japan roadmap for experimental research on corium behavior. *Ann. Nucl. Energy* 124, 541–547.
- Beuzet, E., Lamy, J.S., Bretault, A., Simoni, E., 2011. Modelling of Zry-4 cladding oxidation by air, under severe accident conditions using the MAAP4 code. *Nucl. Eng. Des.* 241 (4), 1217–1224.
- Bratfisch, C., Hoffmann, M., Koch, M. K., 2013. Progress in air ingress simulation with ATHLET-CD. Annual meeting on nuclear technology, Jahrestagung Kerntechnik. Berlin (Germany), 14–16 May 2013.
- Clément, B., Zeyen, R., 2013. The objectives of the Phébus FP experimental programme and main findings. *Ann. Nucl. Energy* 61, 4–10.
- Csordás, A.P., Matus, L., Czitrovsky, A., Jani, P., Maróti, L., Hózer, Z., Windberg, P., Hummel, R., 2000. Investigation of aerosols released at high temperature from nuclear reactor core models. *J. Nucl. Mater.* 282 (2–3), 205–215.
- Dubourg, R., Austregesilo, H., Bals, C., Barrachin, M., Birchley, J., Haste, T., Lamy, J.S., Lind, T., Maliverney, B., Marchetto, C., Pintér, A., Steinbrück, M., Stuckert, J., Trambauer, K., Vimi, A., 2010. Understanding the behaviour of absorber elements in silver–indium–cadmium control rods during PWR severe accident sequences. *Prog. Nucl. Energy* 52 (1), 97–108.
- Durbin, S., Lindgren, E.R., 2017. Investigations of Zirconium Fires during Spent Fuel Pool LOCAs (No. SAND2017-4898PE). Sandia National Lab. (SNL-NM), Albuquerque, NM (United States).
- Duriez, C., Dupont, T., Schmet, B., Enoch, F., 2008. Zircaloy-4 and M5 high temperature oxidation and nitriding in air. *J. Nucl. Mater.* 380 (1–3), 30–45.
- Duriez, C., Steinbrück, M., Ohai, D., Meleg, T., Birchley, J., Haste, T., 2007. Separate Effect Tests on Zirconium Alloy Cladding Degradation in Air Ingress Situations”, 2nd European Review Meeting on Severe Accident Research (ERMSAR-2007), Forschungszentrum Karlsruhe GmbH (FZK), Germany, 12–14 June 2007.
- Gallais-During, A., Bernard, S., Gleizes, B., Pontillon, Y., Bonnin, J., Malgouyres, P.P., Morin, S., Hanus, E., Ducros, G., 2017. Overview of the VERDON-ISTP Program and main insights from the VERDON-2 air ingress test. *Ann. Nucl. Energy* 101, 109–117.
- Giordano, P., Auvinen, A., Brillant, G., Colombani, J., Davidovich, N., Dickson, R., Haste, T., Karkela, T., Lamy, J.S., Mun, C., Ohai, D., Pontillon, Y., Steinbrück, M., Vér, N., 2010. Recent advances in understanding ruthenium behaviour under air-ingress conditions during a PWR severe accident. *Prog. Nucl. Energy* 52 (1), 109–119.
- Grosse, M., Steinbrück, M., Maeng, Y., Sung, J., 2016. Influence of the steam and oxygen flow rate on the reaction of zirconium in Steam/Nitrogen and Oxygen/Nitrogen atmospheres. International Congress on Advances in Nuclear Power Plants, ICAPP 2016 (3), 2103–2111.
- Grosse, M., Pulvermacher, S., Steinbrück, M., Schillinger, B., 2018. In-situ neutron radiography investigations of the reaction of Zircaloy-4 in steam, nitrogen/steam and air/steam atmospheres. *Physica B* 551, 244–248.
- Hofmann, P., 1999. Current knowledge on core degradation phenomena, a review. *J. Nucl. Mater.* 270 (1–2), 194–211.
- Hózer, Z., Windberg, P., Nagy, I., Maróti, L., Matus, L., Horváth, M., Pintér, A., Balaskó, M., Czitrovsky, A., Jani, P., 2003. Interaction of failed fuel rods under air ingress conditions. *Nucl. Technol.* 141, 244–256.
- Lee, J.J., Kim, H.C., 2013. Simulation of Ignition Phenomena in Spent Fuel Assemblies in a Complete Loss-of-Coolant Accident. Transactions of the Korean Nuclear Society Spring Meeting Gwangju.
- Lindgren, E.R., Durbin, S.G., 2007. Characterization of Thermal-Hydraulic and Ignition Phenomena in Prototypic, Full-Length Boiling Water Reactor Spent Fuel Pool Assemblies after a Complete Loss-of-Coolant Accident, NUREG/CR-7143 // SAND2007-2270.
- McCardell, R.K., Russell, M.L., Akers, D.W., Olsen, C.S., 1990. Summary of TMI-2 core sample examinations. *Nucl. Eng. Des.* 118 (3), 441–449.
- Miassoedov, A., Journeau, C., Bechta, S., Hózer, Z., Manara, D., Bottomley, D., Kiselova, M., Langrock, G., 2015. Severe Accident Facilities for European Safety Targets: The SAFEST Project. In: European Review Meeting on Severe Accident Research Conference (ERMSAR), pp. 24–26.
- Mun, C., Cantrel, L., Madic, C., 2006. Review of literature on ruthenium behavior in nuclear power plant severe accidents. *Nucl. Technol.* 156 (3), 332–346.
- Ohnet, M.N., Leroy, O., Mamede, A.S., 2018. Ruthenium behavior in the reactor cooling system in case of a PWR severe accident. *J. Radioanal. Nucl. Chem.* 316 (1), 161–177.
- Perez-Feró, E., Novotny, T., Horváth, M., Kunstar, M., Vér, N., Hózer, Z., 2014. High temperature behaviour of E110G and E110 fuel claddings in various mixtures of steam and air. Proceedings of 2014 water reactor fuel performance meeting, Top fuel, LWR fuel performance meeting. Sendai, Japan, Atomic Energy Society of Japan, 1–4.
- Perez-Feró, E., Pintér-Csordás, A., Novotny, T., Hózer, Z., Illés, L., Radnóczy, Z., 2019. Oxidation of zirconium cladding in air, nitrogen and nitrogen rich steam atmospheres. Proceedings of 2019 Light water reactor fuel performance conference. Seattle, WA. American Nuclear Society, 610–616.
- Pontillon, Y., Geiger, E., Le Gall, C., Bernard, S., Gallais-During, A., Malgouyres, P.P., Hanus, E., Ducros, G., 2017. Fission products and nuclear fuel behaviour under severe accident conditions part 1: Main lessons learnt from the first VERDON test. *J. Nucl. Mater.* 495, 363–384.
- Powers, D.A., Kmetyk, L.N., Schmidt, R.C., 1994. A Review of Technical Issues of Air Ingression during Severe Reactor Accidents, Report NUREG/CR-6218, SAND94-0731, Sandia National Lab.
- Schanz, G., Heck, M., Hózer, Z., Matus, L., Nagy, I., Sepold, L., Stegmaier, U., Steinbrück, M., Steiner, H., Stuckert, J., Windberg, P., 2006. Results of the QUENCH-10 Experiment on Air Ingress, Wissenschaftliche Berichte, FZKA 7087, SAM-LACOMERA-D09, Forschungszentrum Karlsruhe, Institut für Materialforschung, Programm Nukleare Sicherheitsforschung, Mai.
- Shepherd, I., Adroguer, B., Buchmann, M., Gleisberg, O., Haste, T., Hofmann, P., Hózer, Z., Hummel, R., Kaltfofen, R., Knorr, J., Kourt, N., Leonardi, M., Oriolo, F., Schneider, R., Maróti, L., Matus, L., Schanz, G., Windberg, P., 2000. Oxidation Phenomena in Severe Accidents”, Proc. FISA-99, Luxemburg 29 November – 1 December, 1999, EUR 19532 EN, p. 69, G. Van Goethem, J.M. Bermejo, A. Zurita, H. Bischoff, G. Keinhorst, Eds., European Communities.
- Steinbrück, M., 2009. Prototypical experiments relating to air oxidation of Zircaloy-4 at high temperatures. *J. Nucl. Mater.* 392 (3), 531–544.
- Steinbrück, M., 2014. High-temperature reaction of oxygen-stabilized α -Zr(O) with nitrogen. *J. Nucl. Mater.* 447 (1–3), 46–55. <https://doi.org/10.1016/j.jnucmat.2013.12.024>.

- Steinbrück, M., Bottcher, M., 2011. Air oxidation of Zircaloy-4, M5® and ZIRLO™ cladding alloys at high temperatures. *J. Nucl. Mater.* 414 (2), 276–285.
- Steinbrück, M., Miasoedov, A., Schanz, G., Sepold, L., Stegmaier, U., Stuckert, J., 2006. Experiments on air ingress during severe accidents in LWRs. *Nucl. Eng. Des.* 236 (14–16), 1709–1719.
- Stuckert, J., Steinbrück, M., 2014. Experimental results of the QUENCH-16 bundle test on air ingress. *Prog. Nucl. Energ.* 71, 134–141.
- Stuckert, J., Veshchunov, M., 2008. Behaviour of Oxide Layer of Zirconium-Based Fuel Rod Cladding under Steam Starvation Conditions. Scientific report FZKA-7373. <https://doi.org/10.5445/IR/270071587>.
- Stuckert, J., Hózer, Z., Kiselev, A., Steinbrück, M., 2016. Cladding oxidation during air ingress. Part I: Experiments on air ingress. *Ann. Nucl. Energy* 93, 4–17.
- Stuckert, J., Steinbrueck, M., Kalilainen, J., Lind, T., Birchley, J., 2021. Experimental and modelling results of the QUENCH-18 bundle experiment on air ingress, cladding melting and aerosol release. *Nucl. Eng. Design* 379 (2021), 111267. <https://doi.org/10.1016/j.nucengdes.2021.111267>.